Available online at www.sciencedirect.com
ScienceDirect
The Veterinary Journal 177 (2008) 54–62
The Veterinary Journal
www.elsevier.com/locate/tvjl

# Diabetes mellitus-related morphoquantitative changes in the celiac ganglion neurons of the dog

W.L. Guidi [a,✠], J.C.C. Balieiro [b], R.R. De Souza [a], A. Loesch [c], A.A.C.M. Ribeiro [a,*]

[a] *Laboratory of Stereology and Chemical Anatomy, Department of Surgery, College of Veterinary Medicine, University of São Paulo, Av. Prof. Dr. Orlando Marques de Paiva, 87 CEP 02418-160, Brazil*
[b] *Department of Basic Science, College of Food Engineering and Animal Science, University of São Paulo, Pirassununga, CEP: 13.630-970, Brazil*
[c] *Department of Anatomy and Developmental Biology, Hampstead Campus, Royal Free and University College Medical School, University College London, UCL Rowland Hill Street, London NW3 2PF, UK*

Accepted 17 July 2007

**Abstract**

Diabetes mellitus is the most common endocrine disturbance of domestic carnivores and can cause autonomic neurological disorders, although these are still poorly understood in veterinary medicine. There is little information available on the quantitative adaptation mechanisms of the sympathetic ganglia during diabetes mellitus in domestic mammals. By combining morphometric methods and NADPH-diaphorase staining (as a possible marker for nitric oxide producing neurons), type I diabetes mellitus-related morphoquantitative changes were investigated in the celiac ganglion neurons in dogs. Twelve left celiac ganglia from adult female German shepherd dogs were examined: six ganglia were from non-diabetic and six from diabetic subjects.

Consistent hypertrophy of the ganglia was noted in diabetic animals with increase of 55% in length, 53% in width, and 61.5% in thickness. The ordinary microstructure of the ganglia was modified leading to an uneven distribution of the ganglionic units and a more evident distribution of axon fascicles. In contrast to non-diabetic dogs, there was a lack of NADPH-diaphorase perikarial labelling in the celiac ganglion neurons of diabetic animals. The morphometric study showed that both the neuronal and nuclear sizes were significantly larger in diabetic dogs (1.3 and 1.39 times, respectively). The profile density and area fraction of NADPH-diaphorase-reactive celiac ganglion neurons were significantly larger (1.35 and 1.48 times, respectively) in non-diabetic dogs compared to NADPH-diaphorase-non-reactive celiac ganglion neurons in diabetic dogs. Although this study suggests that diabetic neuropathy is associated with neuronal hypertrophy, controversy remains over the possibility of ongoing neuronal loss and the functional interrelationship between them. It is unclear whether neuronal hypertrophy could be a compensation mechanism for a putative neuronal loss during the diabetes mellitus.


*Keywords:* Diabetes mellitus; Celiac ganglion; Dogs; NADPH-diaphorase

## Introduction

Prevertebral sympathetic ganglia are organised in large plexuses, such as the abdominal plexus, which includes the celiac and the cranial mesenteric ganglia that lie close to the abdominal aorta (Gabella, 2004). Miller et al. (1996) defined the celiac ganglia (CG) as an integrator centre of gastrointestinal reflexes from diverse organs, thus recognising its pivotal contribution to gastrointestinal physiology.

It has been demonstrated that the CG may be altered as a result of several types of neuropathy, e.g. diabetic neuropathy, immune neuropathy and degenerative diseases as well as ageing (Schmidt, 1996). In addition, the left celiac ganglion (LCG) is the main source of extrinsic innervation to the pancreas (Miller et al., 1996), which is why it was chosen for the present study.

* Corresponding author. Tel.: +55 113 0911314; fax: + 55 11 30917805.
*E-mail address:* guto@usp.br (A.A.C.M. Ribeiro).
✠ Deceased.

1090-0233/$ - see front matter © 2007 Elsevier Ltd. All rights reserved.
doi:10.1016/j.tvjl.2007.07.012

Diabetes mellitus (DM) is a complex metabolic dysfunction caused either by the inability of the pancreatic islets of Langerhans to secrete insulin or in a deficiency of insulin action at its tissue targets. DM is the most common endocrine disturbance found in domestic carnivores (Nelson, 1998) and, in accordance with its pathogenic mechanisms, is classified in two clinical forms: insulin-dependent (type I DM) and non-insulin dependent (type II DM). Type I DM is more frequent in dogs and usually requires long-term insulin therapy (Nelson, 1998). In cats, however, type II DM is much more common. Type I DM in dogs is characterised by a combination of genetic susceptibility and immunological destruction of beta cells leading to complete insulin insufficiency (Eisenbarth, 1986; Palmer and McCulloch, 1991).

In laboratory animals, several studies have been carried out on either celiac or cranial mesenteric ganglia. These studies have looked at NADPH-diaphorase (NADPH-d) and neuronal nitric oxide synthase (nNOS) expression during spontaneous or induced DM (Schmidt, 1993; Romano et al., 1996; Belai and Burnstock, 1996; Schmidt et al., 2000). NADPH-d has been recognised as a co-enzyme of nitric oxide (NO) production (Palmer et al., 1987; Marletta, 1989; Förstemann et al., 1991; Hope et al., 1991; Vincent and Hope, 1992; Bredt and Snyder, 1992; Marletta, 1993). NO is primarily known as a potent vessel dilator synthesised by NOS from L-arginine and released by the endothelium (Palmer et al., 1987). Some studies have suggested an integration between NO and the vascular endothelium in the development of diabetic neuropathies (Kihara and Low, 1995; Kilo et al., 2000).

Although the pathogenic characteristics of DM and their relationship to NO have been well studied, particularly in rats and humans, there is still little information on the quantitative adaptation mechanisms of the autonomic nervous system during DM in domestic mammals. By combining morphometric and histochemical techniques, we investigated the interrelation between NO-associated neurons and type I DM in dogs in an attempt to provide a morphofunctional insight into diabetic neuropathy in animals of veterinary interest.

## Materials and methods

### *Animals*

Twelve LCG from adult female German shepherd dogs were investigated. Six ganglia came from a non-diabetic group (group I) and six from spontaneous diabetic dogs (group II). The experiments were approved by the Animal Care Commission of the Department of Surgery of the College of Veterinary Medicine of University of São Paulo (protocol number 193/2002). It should be stressed that the euthanasia of diabetic female dogs was officially authorised by the owners. All procedures were undertaken on animals coming to our hospital for diagnosis and clinical or surgical treatments.

Group I animals had bodyweights ranging from 21 to 25 kg (mean = 23.3 kg; SD = 1.5) and they were aged 35–37 months on the day of euthanasia. Animals from group II had bodyweights varying between 23 and 27 kg (mean = 25.7 kg; SD = 1.7) and they were aged 39–42 months on the day of euthanasia. The animals were not related to each other, either within groups or between groups.

For each dog, a detailed set of information was recorded, including age, bodyweight, and clinical and laboratory test results to determine whether it was non-diabetic or diabetic.

Animals were considered non-diabetic when they presented no clinical symptoms of DM (Group I), and showed normoglycaemia on five consecutive monthly tests. In contrast, dogs from group II were defined as presenting with chronic type I DM when hyperglycaemia (>250 mg/dL) and glucosuria were observed simultaneously with polyuria, polyphagia, polydipsia and eventually loss of bodyweight (Feldman and Nelson, 2004; Catchpole et al., 2005).

Type I DM dogs were diagnosed at age 29–31 months and were under therapy with human insulin (1 mg; 2.7 units/kg/twice a day) for a period of 10 months. Animals were controlled for the whole treatment period and tested each month for evidence of hyperglycaemia. The levels of blood glucose were on average always over 250 mg/dL, which is higher than for non-diabetic animals. These dogs had no history of any previous treatment and their conditions were not related to the stage of ovarian cycle.

Group I (non-diabetic animals) and Group II (diabetic animals) were further divided into two subgroups, IA and IIA – for the morphometric study, and IB and IIB – for the histochemical study of NADPH-d-positive neurons. Subgroups IA and IIA consisted of three LCG each, and subgroups IB and IIB also possessed three LCG each.

### *Laboratorial examinations*

Blood glucose levels were determined using a portable glucose meter (Medisense Optium Abbott Laboratories). Urine glucose determination was performed using a test strip (Dipstick – Combur UX, Roche Diagnostics) (Willard et al., 1994).

### *Histology*

After euthanasia, the abdominal cavity was opened by a midline incision. Abdominal organs such as stomach, intestines and adrenal were moved aside to facilitate the identification of the ganglia and their connections to the spinal cord, and also to facilitate the visualization of the intermesenteric plexus and main vessels of the abdomen (abdominal aorta and caudal cava vein).

Approximately 100 mL of phosphate-buffered saline (PBS) (Sigma) (0.1 M; pH 7.4) containing 2% heparin (Roche) and 0.1% sodium nitrite (Sigma) were perfused through the abdominal aorta close to the emergence of the celiac artery. The caudal vena cava was cut to empty the circulatory system. This was followed by the perfusion of 100 mL fixative consisting of 5% glutaraldehyde (Merck) and 1% formaldehyde (Sigma) in sodium cacodylate buffer (EMS) (0.125 M; pH 7.4) (for animals from subgroups IA and IIA) or 4% formaldehyde in PBS (for animals from subgroups IB and IIB).

The LCG were dissected out together with their connections to the left major splanchnic nerve and the intermesenteric and celiac plexus. Then the ganglia were immersion-fixed in the same fixative for 2–3 days at 4 °C. Perfusion-fixed (wet) ganglia were measured for length, width and thickness using a digital pachymeter (Digimess).

Ganglia from subgroups IA and IIA were washed in sodium cacodylate buffer (EMS), post-fixed in 2% osmium tetroxide (EMS), block-stained with a uranyl acetate saturated aqueous solution (Reagen), dehydrated in graded ethanol and propylene oxide (EMS) and embedded in Araldite (502 Polyscience). The resin was cured at 60 °C for 3 days. Sections, 2 μm thick, were cut from the Araldite-embedded specimens using a glass knife. These were then stained with toluidine blue (nuclear), dried on a hot plate and mounted under a cover slip with a drop of Araldite.

### *Morphometry*

Each ganglion was exhaustively cut and for the morphometric study 70–80 serial sections were cut, each 2 μm thick. For each ganglion, 30

consecutive sections were collected on glass slides, stained with toluidine blue and mounted in Araldite. A test-system comprising eight unbiased counting frames was placed over each section and projected on a computer screen. The total sampled area (a) in the test-systems was 40,000 μm$^2$.

A fraction (1/fr) of the counting frames was random uniform and systematically sampled (SURS) using a random start between 1 and fr. The sampled field's images were observed on a computer screen using a Leica DMR Microscope coupled with a DFC 300FX Leica digital camera. In each counting frame (with a surrounding guard area), only the neurons located inside the counting frame and not on the forbidden lines were measured (Gundersen, 1977). This approach was also adopted in a 3-D view "brick counting frame" (Howard and Reed, 2005).

Each neuron received the same number in all serial sections, and its largest perikaryon profile as well as its largest nuclear-profile were identified and therefore measured for the cross-sectional area using the image analysis system Q-Win Leica. In each animal group, a total of 150 neurons (50 neurons per ganglion) and 120 neuronal nuclei (40 nuclei per ganglion) were measured.

### *Histochemistry*

The collected ganglia from subgroups IB and IIB were kept for 2–3 days at 4 °C in the fixative (see details above). The samples were then transferred to a cryoprotection solution composed of PBS and 20% sucrose and stored overnight at 4 °C. Next, ganglia were coated with Tissue Tek, immersed in isopentane pre-cooled with liquid nitrogen. This was exhaustively cut at 30 μm in a Leica cryostat, mounted on glass slides coated with poly-L-lysine and stored in a freezer at −20 °C for 2–3 days, according to the protocol published by Scherer-Singler et al. (1983), Santer and Symons (1993) and Atoji et al. (2000) to identify NADPH-d activity in autonomic neurons.

### *NADPH-d staining*

Slides were washed three times in PBS for 10 min and incubated in a mixture of β-NADPH (1 mg/mL), nitroblue tetrazolium (NBT – 0.25 mg/mL) and 0.3% triton X-100 in PBS for 60 min at 37 °C. Control staining was carried out by incubating the slides in a medium free of β-NADPH. The histochemical staining of all investigated sections from subgroups IB and IIB was simultaneously performed and using the same incubation protocol.

### *Profile density ($Q_A$) of NADPH-d-reactive and NADPH-d-non-reactive neurons*

The density of cell profiles in a given area (profile or packing density) was estimated using the following formula (Howard and Reed, 2005):

$Q_A = \Sigma$ profiles/given area.

A test-system comprising eight unbiased counting frames was placed over each section field's image projected on a computer screen. The total sampled area ($a$) in the test-systems was 40,000 μm$^2$.

### *Area fraction ($A_A$) of NADPH-d-reactive neurons and NADPH-d-non-reactive neurons*

Area fraction ($A_A$) represents the fraction of total LCG area occupied by NADPH-d-reactive and NADPH-d-non-reactive neurons obtained by randomly throwing a point grid system over a given section. Next, the total number of points falling within the reference space was counted ($P_{(rs)}$) as was the total number of points landing on neuronal cell bodies ($P_{(cb)}$). Then, $A_A$ was estimated as: $A_A = \sum P_{(cb)}/\sum P_{(rs)}$. The results were expressed as a percentage (Howard and Reed, 2005).

### *Statistical analysis*

For continuous distribution data (ganglion measurements, cell area and nuclear area), the analysis accounted for the comparative effect between groups (diabetic and non-diabetic dogs), using General Linear Models (GLM) ($F$-test), through the PROC GLM procedure of the Statistical Analysis System software, version 8.02 (SAS, 1995). In case of significant data ($P < 0.05$), Student's $t$ test was applied for multiple comparisons. For cell counting (discrete distribution data), i.e. cell profile density and cell area fraction, the same comparative effect between groups (diabetic and non-diabetic dogs) was considered, though using a Generalised Linear Method, assuming a Poisson distribution with logarithmic linking function through the PROC GENMOD procedure of the same software. In case of significant data ($P < 0.05$), the Chi-square test was used for multiple comparisons.

## Results

The results are shown as means (CV). CV is SD/mean.

In all animals examined the LCG was irregular in shape and this was particularly apparent in diabetic subjects. The LCG was located close to the abdominal aorta involving the emergence of the celiac artery. The dorsal portion of the ganglion was connected to the thoracic sympathetic trunk by the left major splanchnic nerve and its caudal portion to the cranial mesenteric ganglion through interganglionic nerves.

Perfusion-fixed (wet tissue) and not-fresh ganglia were measured and the same procedure was performed in the two groups for comparative purposes. Hence, the ganglion length, width and thickness were 9.02 mm (0.1), 4.5 mm (0.04) and 2.6 mm (0.1), respectively, for non-diabetic animals and 14.3 mm (0.2), 6.9 mm (0.05) and 4.2 mm (0.1), respectively, for diabetic dogs. The results were different ($P < 0.05$).

In general, the LCG microstructure was represented by a ganglionic mass surrounded by a capsule containing connective tissue and vessels. The capsule sent connective tissue septa inside the ganglion and divided it into ganglionic units composed of various cell types, i.e. ganglion neurons (organised in tight clusters), glial cells and small intensely fluorescent (SIF) cells. Ganglionic units were separated from each other by nerve fibres, intraganglionic capillaries and septa of collagen fibres (Fig. 1A). A visible DM-related change was the non-homogeneous distribution of neuronal clusters when compared to the almost homogeneous distribution in non-diabetic subjects. Nerve cell bodies were far apart and the large spaces between them were occupied mainly by axon fascicles (Fig. 1B). The ganglion capsule thickness was 17.2 μm (0.20) in non-diabetic dogs and 26.9 μm (0.15) in diabetic animals. Differences between groups were significant ($P < 0.05$).

### *Cell size*

The neuronal cross-sectional area was 781.3 μm$^2$ (0.39) in non-diabetic dogs and 1,039.4 μm$^2$ (0.28) in diabetic dogs. Mean values were significant between groups ($P < 0.05$, Fig. 2). In non-diabetic subjects, the majority of neurons had a cross-sectional area varying from 500 to 900 μm$^2$ (43.3%), whereas in diabetic dogs 49.9% of neu-

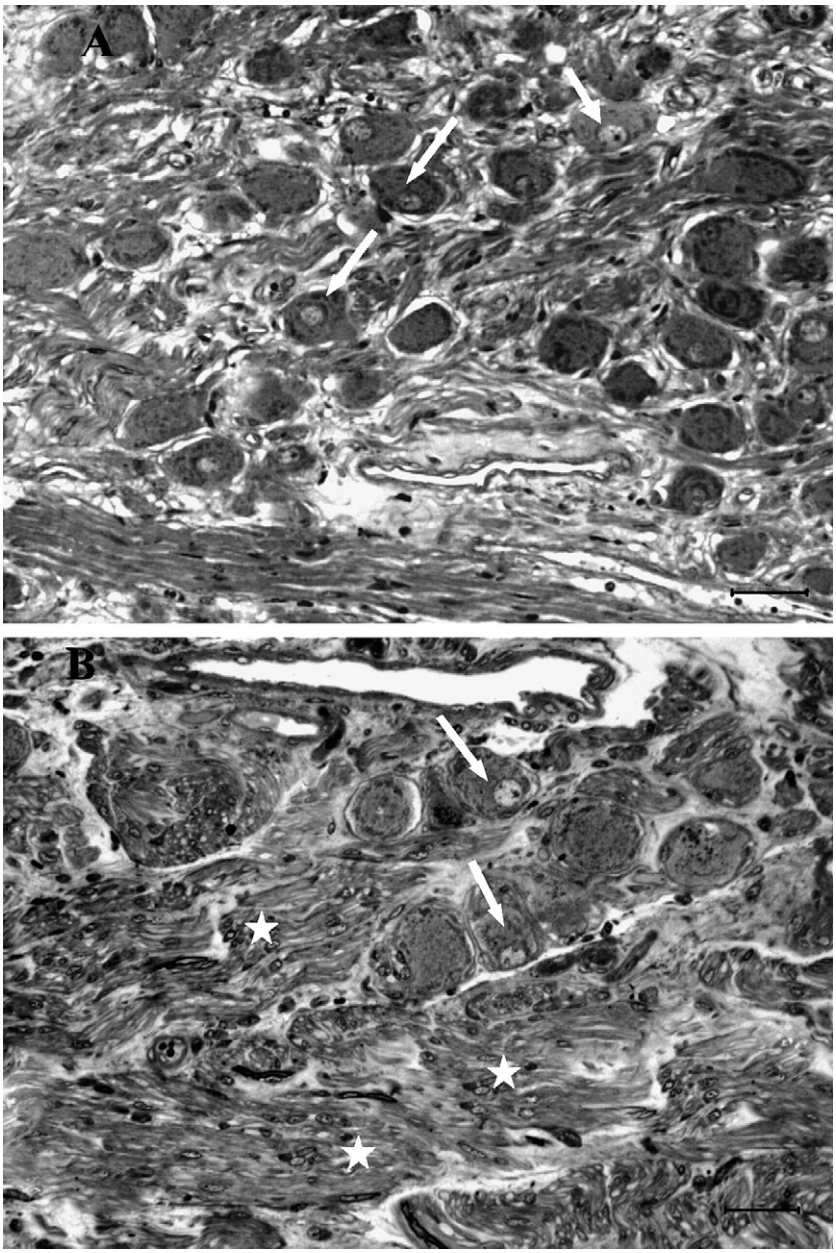


Fig. 1. Fine structure of the celiac ganglion of a non-diabetic (A) and a diabetic dog (B) in semi-thin sections photographed at the same magnification. Note the homogeneous distribution of ganglion neurons (arrows) in non-diabetic (A) when compared to the non-homogeneous pattern (arrows) in diabetic subjects (B). In the ganglion of diabetic dogs the nerve cell bodies are separated by large spaces occupied mainly by axon fascicles (★). Toluidine blue. Calibration bar: 40 μm.

rons had a cross-sectional area varying from 900 to 1300 $\mu m^2$.

*Nuclear size*

The nuclear cross-sectional area was 76.7 $\mu m^2$ (0.60) in non-diabetic dogs and 106.7 $\mu m^2$ (39.7) in diabetic animals. The differences between groups were significant ($P < 0.05$, Fig. 3). In non-diabetic animals, the majority of neurons had a nuclear cross-sectional area varying from 10 to 70 $\mu m^2$ (54.1%), whereas in diabetic dogs 54.2% of neurons had a cross-sectional area varying from 70 to 130 $\mu m^2$.

*NADPH-d staining*

Differences in NADPH-d perikaryal staining were observed between non-diabetic and diabetic dogs, namely a loss of neuronal cell body staining in the latter (Fig. 4A and B). The profile density ($Q_A$) of NADPH-d-reactive and NADPH-d-non-reactive neurons was $27.5 \times 10^{-5}$ $\mu m^{-2}$ (0.12) in non-diabetic dogs and $20.3 \times 10^{-5}$ $\mu m^{-2}$ (0.19) in diabetic animals (Fig. 4A and B). Differences between groups were significant ($P < 0.05$). The area fraction ($A_A$) of NADPH-d-reactive and NADPH-d-non-reactive celiac ganglion neurons was 61% (0.12) in non-diabetic

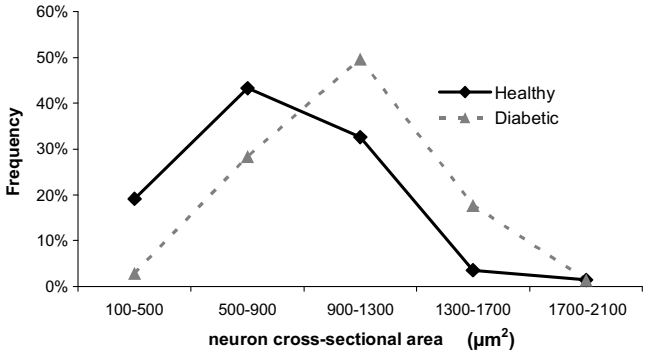


Fig. 2. Line-graph documenting the percentage distribution of neuronal sizes (cross-sectional area of the largest profile of a neuron) divided into classes of the same size for both non-diabetic and diabetic dogs and ranging from the lowest (100–500 μm$^2$) to the largest (1700–2100 μm$^2$). A shift to the right and an increased neuronal cross-sectional area is evident in the diabetic dogs.

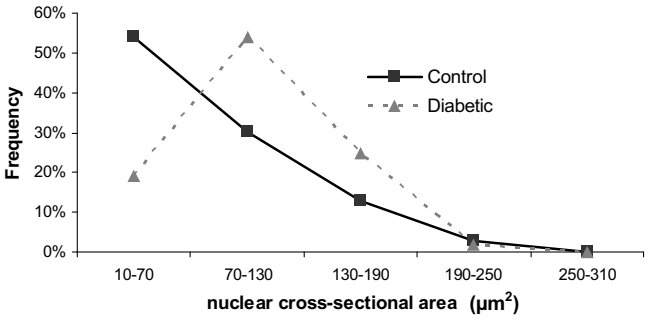


Fig. 3. Line-graph documenting the percentage distribution of neuronal nuclear sizes (cross-sectional area of the largest profile of a neuron nucleus) divided into classes of the same size for both non-diabetic and diabetic dogs and ranging from the lowest (10–70 μm$^2$) to the largest (250–310 μm$^2$). A shift to the right and an increased nuclear cross-sectional area is evident in the diabetic dogs.

dogs and 43% (0.22) in diabetic subjects. Mean values were significantly different between groups ($P < 0.05$).

## Discussion

Independently from the specific group analysed in this study, the localisation of the LCG was quite similar in both non-diabetic and diabetic dogs. The LCG was separated from the cranial mesenteric ganglion in all dogs in contrast to the study pursued by Hammer and Santer (1981) and Ghoshal (1986) which reported that the LCG was located over the celiac artery. As with Promwikorn et al. (1998), a very irregular shape of LCG was noticed in both groups, although it was more prominent in diabetic animals. In this sense, our results are quite different from those reported in the literature, i.e. those describing a semi-lunar shape in rats (Gabella, 2004) and a plexiform nature in dogs (Mizeres, 1955). In addition, in our study a consistent ganglion hypertrophy was seen in diabetic dogs, i.e. 55% in length; 53% in width and 61.5% in thickness.

In non-diabetic dogs, LCG microstructure was quite similar to that previously reported by Ribeiro et al. (2002) in dogs, by Sasahara et al. (2003) for rabbits, Ribeiro et al. (2004) for rats, capybaras and horses, and Schmidt (1996) for humans. In general, the connective tissue of the ganglionic capsule sends out connective septa inside the LCG dividing the parenchyma into ganglionic units. Each unit is made up of three elements: ganglion neurons, glial cells and SIF cells. In addition, capillaries were observed within the parenchyma and were therefore classified here as inter-unit and intra-unit capillaries.

A similar vascular classification was adopted by DePace (1981), Abe et al. (1983), Chau et al. (1991), Mascorro et al. (1995) and Chau and Lu (1995). However, this regular microstructure was modified in diabetic dogs, i.e. a remarkable non-homogeneous distribution of ganglionic units which was accompanied by a 29.5% increase in non-neuronal ganglionic tissue, namely axon fascicles. In addition, a 56.4% increase in the ganglion's capsule thickness was noticed. A comparable pattern was reported by Schmidt et al. (1993) in diabetic humans.

Some additional DM-related changes such as lymphocyte infiltration and vacuolated neurons were not observed in the diabetic dogs, though they have been reported in humans (Duchen et al., 1980; Schmidt, 1996). Furthermore, in the diabetic dogs, axonal degeneration and loss of either sympathetic or parasympathetic unmyelinated post-ganglionic fibres were not seen although these have been reported in cats (Post and McLeod, 1977a,b) and in humans (Schmidt, 1993). In fact, the main effect of DM on the autonomic nervous system is the axonal dystrophy of pre-vertebral ganglia (human and rat), manifested by pre-terminal axonal dilatation and an atypical synaptic morphology (Schmidt et al., 1983, 1992; Schmidt and Plurad, 1986). Structural changes were also reported within axon varicosities of enteric nervous system of experimental diabetic rats (Loesch et al., 1986).

The neuronal size (cross-sectional area) of LCG was significantly larger (1.3-fold) in diabetic dogs. A similar neuronal hypertrophy (increased cell long axis) was also reported for the cranial mesenteric and cranial cervical ganglia of diabetic rats (Schmidt et al., 1983). Moreover, a significant increase in nuclear size (1.39-fold) was noticed in LCG neurons of diabetic dogs in this study. This agrees with the finding by Nadelhaft et al. (1993), i.e. that average sizes of neurons in major pelvic, dorsal root, caudal mesenteric and sympathetic chain ganglia were significantly larger (from 13 to 68%) in streptozotocin-induced diabetic rats. However, these authors also reported no size differences in the cranial cervical ganglion neurons between control and diabetic animals, which contradicted the findings of neuronal hypertrophy detected by Schmidt et al. (1983) and the present study.

Although an increase in cell body size was verified in our study, the neuronal shape was unaltered in diseased ani-

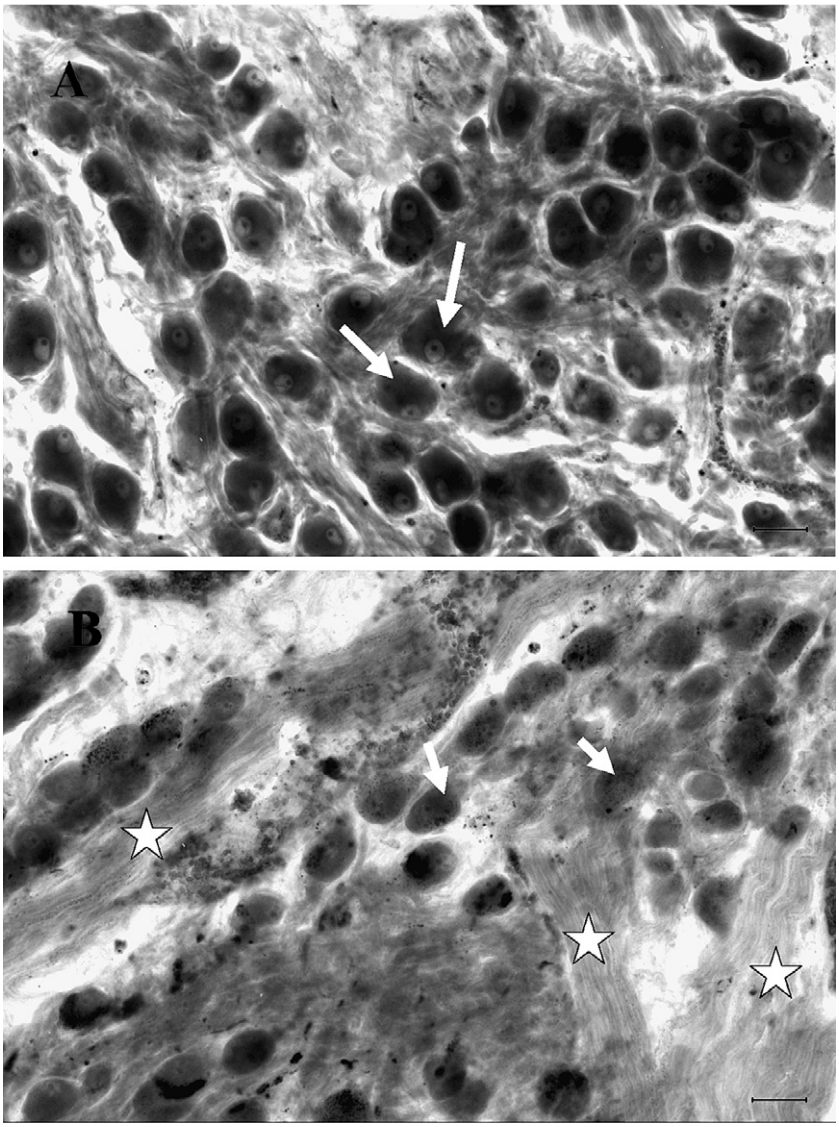


Fig. 4. Microstructure of the celiac ganglion's NADPH-d reactive neurons (arrows) of a non-diabetic (A) and NADPH-d-non-reactive neurons of a diabetic dog (B) in cryosections photographed at the same magnification. The non-homogeneous distribution of celiac ganglion neurons (arrows) in diabetic subjects leads to a smaller profile density. Also, note axon fascicles (★) and lack of NADPH-diaphorase labelling (arrows) in diabetic dogs. Calibration bar: 40 μm.

mals, in disagreement with Schmidt (1996, 2001) who reported deformations in the neuronal cell bodies of sympathetic ganglia from diabetic humans and rats. Schmidt et al. (1983) and Schmidt and Plurad (1986) reported that there was no evidence of significant loss of neurons, or a difference in mean diameter of principal sympathetic ganglion neurons in the cranial cervical ganglion in DM compared with control values, although there was a hint of a shift to larger neuronal diameters. Furthermore, no significant reductions in nerve cell size in either cranial cervical or cranial mesenteric ganglia of human diabetic subjects have been reported (Schmidt et al., 1993). The differences between our findings and other results may be related to the fixation method and perfusion pressure used and the type of size measurement pursued, i.e., Schmidt et al. (1993) used a linear measurement (diameter) whereas we estimated neuronal profile sizes using 2-D areal measurements, which are more accurate than linear approaches to size estimates.

As to the non-significant loss of neurons reported by Schmidt et al. (1983) and Schmidt and Plurad (1986), it is clear that they did not used 3-D design-based stereological methods and, therefore were not entitled to report on the number of neurons. For this reason we reported on the number of neuronal profiles per area and not on the number of neurons.

In the present study a differential NADPH-d perikaryal staining was observed between non-diabetic and diabetic dogs, namely lack of staining in diabetic dogs. In agreement with our findings, a lack of NADPH-d staining was also reported by Schmidt et al. (1993) for the prevertebral cranial mesenteric ganglia of diabetic rats. However, no

differences were observed between non-diabetic and diabetic animals in the NADPH-d staining pattern in the cranial cervical ganglion. It might therefore be assumed that different autonomic ganglia differentially react in diabetic conditions. It should be mentioned that NAPDH-d staining is an indirect labelling of dehydrogenases and NOS isoforms, including nNOS (Lincoln et al., 1997) and has been used to label putative NO-producing neurons (e.g. Schmidt, 1993; Romano et al., 1996; Belai and Burnstock, 1996; Schmidt et al., 2000). NOS may also be an NADPH-d (Hope et al., 1991) and the extensive co-localisation of reactivity of the two enzymes in various tissues including brain, adrenals, kidneys and gut is well established (Dawson et al., 1991; Bredt and Snyder, 1992). However, the co-localisation of NOS immunoreactivity with the NADPH-d reaction does not mean that the two enzymes are the same (Lincoln et al., 1997). This lack of certainty may be relevant to unfixed biological tissues (Tracey et al., 1993). On the other hand, more reliable NADPH-d staining can be used to demonstrate NOS when the tissues have been fixed with formaldehyde/paraformaldehyde (Afework et al., 1992; Hassall et al., 1992; Saffrey et al., 1992; Nakos and Gossrau, 1994; Worl et al., 1994), as was in the case in our study.

The area fraction and the number of NADPH-d reactive and NADPH-d-non-reactive neuronal profiles per area were investigated comparatively between non-diabetic and diabetic dogs, respectively. The profile density of the NADPH-d-reactive LCG neurons was significantly larger (1.35-fold) in non-diabetic dogs. Similarly, the area fraction of those neurons was significantly increased by 1.48-fold in non-diabetic dogs. By taking the two parameters together, i.e. profile density and area fraction, and combining them with the nerve cell size, one may infer that the decrease of profile density and area fraction might be related to the increase in nerve cell size as a result of DM. Furthermore, Schmidt et al. (1993) have reported a 14% significant decrease ($P = 0.04$) in the neuronal profile density in the superior mesenteric ganglion but not in the superior cervical ganglion of diabetic human patients. Several papers have reported that long-term DM (10 months) in man caused no substantial loss of neurons (as measured by the neuron density/mm$^2$) (Schmidt et al., 1983; Schmidt and Plurad, 1986).

More recently, Schmidt (2001) reported that 10 months of severe untreated experimental DM failed to produce both significant neuron loss and decrease in neuronal density in either rat cranial mesenteric or cranial cervical ganglia. These results do not support the hypothesis that apoptosis would be involved in the pathogenesis of diabetic neuropathy and would therefore lead to a loss of significant numbers of neurons as a characteristic finding of experimental streptozotocin-induced diabetic autonomic neuropathy (Appenzeller and Richardson, 1966; Duchen et al., 1980; Russell and Feldman, 1999; Russell et al., 1999). Several hypotheses have been proposed to explain the pathogenesis of diabetic neuropathy. One of these shows a similarity between age- and DM-related sympathetic system damage, suggesting the potential for shared pathogenic mechanisms in experimental DM and ageing (Schmidt and Plurad, 1986; Schmidt et al., 1989 and Schroer et al., 1992).

## Conclusions

Although it is widely known that diabetic neuropathy causes a neuronal hypertrophy as reported in the literature, there is still controversy over whether it leads to a decrease in the total number of neurons in sympathetic ganglia. Few studies have been undertaken using design-based stereological methods to address this crucial question. Thus, several aspects remain unclear, namely, (1) is there any neuronal loss during the process? (2) If there is a neuronal loss, might it be compensated for by the neuronal hypertrophy as postulated by Cabello et al. (2002) for the substantia nigra in humans? Further 3-D unbiased quantitative investigations of the total number of neurons are necessary to shed light on this point. An increased understanding is crucial to both the treatment and the prognostics of DM in veterinary medicine.

## Acknowledgments

We wish to dedicate this article to the memory of Wanderley Lima Guidi, whom we very much miss as a most dedicated and good scientist, colleague and friend. We would also like to thank K.M. Gagliardo and E.T. Fioretto for their assistance.

## References

Abe, H., Watanabe, H., Yamamoto, T.Y., 1983. Relationship between granule-containing cells and blood vessels in the rat autonomic ganglia. Anatomical Record 205, 65–72.

Afework, M., Tomlinson, A., Belai, A., Burnstock, G., 1992. Colocalization of nitric oxide synthase and NADPH-diaphorase in rat adrenal gland. Neuroreport 3, 893–896.

Appenzeller, O., Richardson, E.P., 1966. The sympathetic chain in patients with diabetic and alcoholic polyneuropathy. Neurology 16, 1205–1209.

Atoji, Y., Mizutani, K., Yamamoto, Y., Suzuki, Y., 2000. Innervation of the pigeon oviduct: correlation of NADPH diaphorese with acetylcholinesterase, tyrosine hydroxylase and neuropeptides. Autonomic Neuroscience 84, 1–7.

Belai, A., Burnstock, G., 1996. Acrylamide-induced neuropathic changes in rat enteric nerves: Similarities with effects of streptozotocin-diabetes. Journal of Autonomic Nervous System 58, 56–62.

Bredt, D.S., Snyder, S.H., 1992. Nitric oxide, a novel neuronal messenger. Neuron 8, 3–11.

Cabello, C.R., Thune, J.J., Pakkenberg, H., Pakkenberg, B., 2002. Ageing of substantia nigra in humans: cell loss may be compensated by hypertrophy. Neuropathology and Applied Neurobiology 28, 283–291.

Catchpole, B., Ristic, J.M., Fleeman, L.M., Davison, L.J., 2005. Canine diabetes mellitus: can old dogs teach us new tricks?. Diabetologia 48 1948–1956.

Chau, Y.P., Lu, K.S., 1995. Investigation of the blood-ganglion barrier properties in rat sympathetic ganglia by using lanthanum ion and horseradish peroxidase as tracers. Acta Anatomica 153, 135–144.

Chau, Y.P., Chien, C.L., Lu, K.S., 1991. The permeability of capillary among the small granule-containing cells in rat superior cervical ganglia: an ultrastructural lanthanum tracer study. Histology Histopathology 6, 261–268.

Dawson, T.M., Bredt, D.S., Fotuhi, M., Hwang, P.M., Snyder, S.H., 1991. Nitric oxide synthase and neuronal NADPH diaphorase are identical in brain and peripheral tissues. Proceedings National Academy of Science. USA 88, 7797–7801.

DePace, D.M., 1981. Morphologic study of the blood vessels of the superior cervical ganglion of the albino rat. Acta Anatomica 109, 238–246.

Duchen, L.W., Anjorin, S., Watkins, P.J., Mackay, J.D., 1980. Pathology of autonomic neuropathy in diabetes. Annals International of Medicine 92, 301–303.

Eisenbarth, G.S., 1986. Type I diabetes mellitus. A chronic autoimmune disease. The New England Journal of Medicine 314, 1360–1368.

Feldman, E.C., Nelson, R.W., 2004. Canine diabetes mellitus. In: Canine and Feline Endocrinology and Reproduction, third ed. WB Saunders, Philadelphia, pp. 486–538.

Förstemann, U., Schmidt, H.H.H.W., Pollock, J.S., Sheng, H., Mitchell, J.A., Warner, T.D., Nakane, M., Murad, F., 1991. Isoforms of nitric oxide synthase. Characterization and purification from different cell types. Biochemical Pharmacology 42, 1849–1857.

Gabella, G., 2004. The Rat autonomic Nervous System, third ed. Elsevier, pp. 77–99.

Ghoshal, N.G., 1986. Inervação autônoma abdominal, pélvica e caudal. In: Getty, R. (Ed.), Sisson e Grossman Anatomia dos Animais Domésticos, fifth ed. Guanabara Koogan, pp. 650–654.

Gundersen, H.J.G., 1977. Notes on the estimation of the numerical density of arbitrary profiles: the edge effect. Journal of Microsciences 111, 219–223.

Hammer, D.W., Santer, R.M., 1981. Anatomy and blood supply of celiac-superior mesenteric ganglion complex of the rat. Anatomy and Embryology 162, 353–362.

Hassall, C.J., Saffrey, M.J., Belai, A., Hoyle, C.H.V., Moules, E.W., Moss, J., Schmidt, H.H.H.W., Murad, F., Förstermann, U., Burnstock, G., 1992. Nitric oxide synthase immunoreactivity and NADPH-diaphorase activity in a subpopulation of intrinsic neurons of the guinea pig heart. Neuroscience Letters 143, 65–68.

Hope, B.T., Michael, G.J., Knigee, K.M., Vincent, S.R., 1991. Neuronal NADPH-diaphorese is a nitric oxide synthase. Proceedings of National Academy of Science USA 88, 2811–2814.

Howard, C.V., Reed, M.G., 2005. Unbiased StereologyThree Dimensional Measurement in Microscopy. BIOS Scientific Publishers.

Kihara, M., Low, P.A., 1995. Impaired vasoreactivity to nitric oxide in experimental diabetic neuropathy. Experimental Neurology 132, 180–185.

Kilo, S., Berghoff, M., Hilz, M., Freeman, R., 2000. Neural and endothelial control of the microcirculation in diabetic peripheral neuropathy. Neurology 54, 1246–1252.

Lincoln, J., Hoyle, C.H.V., Burnstock, G., 1997. Nitric Oxide in Health and Disease. Cambridge University Press.

Loesch, A., Belai, A., Lincoln, J., Burnstock, G., 1986. Enteric nerves in diabetic rats: electron microscopic evidence for neuropathy of vasoactive intestinal polypeptide-containing fibres. Acta Neuropathologica 70, 161–168.

Marletta, M.A., 1989. Nitric oxide: biosynthesis and biological significance. Trends in Biochemical Sciences 14, 488–492.

Marletta, M.A., 1993. Nitric oxide synthase structure and mechanism. Journal of Biological Chemistry 268, 12231–12234.

Mascorro, J.A., Breaux, T.F., Yates, R.D., 1995. Morphological observations of small granule containing (chromaffin) cells in the celiac ganglion of the guinea-pig, with emphasis on cell contacts. Microscopic Research and Technique 29, 169–176.

Miller, S.M., Hanani, M., Kuntz, S.M., Schmalz, P.F., Szurszewski, J.H., 1996. Light, electron and confocal microscopic study of the mouse superior mesenteric ganglion. Journal of Comparative Neurology 365, 427–444.

Mizeres, N.J., 1955. The anatomy of the autonomic nervous system in the dog. American Journal of Anatomy 96, 285–317.

Nadelhaft, I., Vera, P.L., Steinbacher, B., 1993. Hypertrophic neurons innervating the urinary bladder and colon of the streptozotocin-diabetic rat. Brain Research 609, 277–283.

Nakos, G., Gossrau, R., 1994. When NADPH-diaphorase (NADPH-d) works in the presence of formaldehyde, the enzyme appears to visualize selectively cells with constitutive nitric oxide synthase (NOS). Acta Histochemica 96, 335–343.

Nelson, R.W., 1998. Diabetes Melito. In: Birchard, Scherding Manual Saunders, first ed. Ed. Roca, São Paulo, Brasil, pp. 283–291.

Palmer, R.M., Ferrige, A.G., Moncada, S., 1987. Nitric oxide release accounts for the biological activity of endothelium-derived relaxing factor. Nature 327, 524–526.

Palmer, J.P., McCulloch, D.K., 1991. Prediction and prevention of IDDM – 1991. Diabetes 40, 943–947.

Post, E.J., McLeod, J.G., 1977a. Acrylamide autonomic neuropathy in the cat, Part 1. Neurophysiological and histological studies. Journal of Neurological Science 33, 353–374.

Post, E.J., McLeod, J.G., 1977b. Acrylamide autonomic neuropathy in the cat, Part 2. Effects on mesenteric vascular control. Journal of Neurological Science 33, 375–385.

Promwikorn, W., Thongpila, S., Pradidarcheep, W., Mingsakul, T., Chunhabundit, P., Somana, R., 1998. Angioarchitecture of the celiac sympathetic ganglion complex in the common tree shrew (*Tupaia glis*). Journal of Anatomy 193, 409–416.

Ribeiro, A.A.C.M., Davis, C., Gabella, G., 2004. Estimate of size and total number of neurons in superior cervical ganglion of rat, capybara and horse. Anatomy and Embryology 208, 367–380.

Ribeiro, A.A.C.M., Elias, C.F., Liberti, E.A., Guidi, W.L., De Souza, R.R., 2002. Structure and ultrastructure of the celiac mesenteric ganglion complex in the domestic dog. Anatomia Histologia Embryologia 31, 344–349.

Romano, B.E., de Miranda Neto, H.M., Cardoso, S.R.C., 1996. Preliminary investigation about the effects of the streptozotocin-induced chronic diabetes on the nerve cell number and size of myenteric ganglia in rat colon. Revista Chilena Anatomia 14, 139–145.

Russell, J.W., Feldman, E.L., 1999. Insulin-like growth factor-I prevents apoptosis in sympathetic neurons exposed to high glucose. Hormone Metabolism Research 31, 90–96.

Russell, J.W., Sullivan, K.A., Windebank, A.J., Herrmann, D.N., Feldman, E.L., 1999. Neurons undergo apoptosis in animal and cell culture models of diabetes. Neurobiological Disorders 6, 347–363.

Saffrey, M.J., Hassall, C.J., Hoyle, C.H., Belai, A., Moss, J., Schmidt, H.H., Forstermann, U., Murad, F., Burnstock, G., 1992. Colocalization of nitric oxide synthase and NADPH-diaphorase in cultured myenteric neurones. Neuroreport 4, 333–336.

Santer, R.M., Symons, D., 1993. Distribution of NADPH-diaphorese activity in rat paravertebral, prevertebral and pelvic sympathetic ganglia. Cell Tissue Research 271, 115–121.

Sasahara, T.H.C., Souza, R.R., Machado, M.R.F., Silva, R.A., Guidi, W.L., Ribeiro, A.A.C.M., 2003. Macro- and microstructural organization of the rabbit′ s celiac-mesenteric ganglion complex (*Oryctolagus cuniculus*). Annals of Anatomy 185, 441–448.

Scherer-Singler, U., Vincent, S.R., Kimura, H., McGeer, E.G., 1983. Demonstration of a unique population of neurons with NADPH-diaphorase histochemistry. Journal of Neuroscience Methods 9, 229–234.

Schmidt, R.E., 1996. The neuropathology of human sympathetic autonomic ganglia. Microscopic Research and Technique 35, 107–121.

Schmidt, R.E., 1993. The role of nerve growth factor in the pathogenesis and therapy of diabetic neuropathy. Diabetic Medicine 10 (Suppl. 2), 10s–13s.

Schmidt, R.E., 2001. Neuronal preservation in the sympathetic ganglia of rats with chronic streptozotocin-induced diabetes. Brain Research 921, 256–259.

Schmidt, R.E., Plurad, S.B., 1986. Ultrastructural and biochemical characterization of autonomic neuropathy in rats with chronic streptozotocin diabetes. Journal of Neuropathology Experimental Neurology 45, 525–544.

Schmidt, R.E., Plurad, S.B., Modert, C.W., 1983. Experimental diabetic autonomic neuropathy – characterization in streptozotocin-diabetic Sprague-Dawley rats. Lab Invest 49, 538–552.

Schmidt, R.E., Dorsey, D.A., Roth, K.A., 1992. Immunohistochemical characterization of NPY and substance P containing nerve terminals in aged and diabetic human sympathetic ganglia. Brain Research 583, 320–326.

Schmidt, R.E., Plurad, S.B., Parvin, C.A., Roth, K.A., 1993. The effects of diabetes and aging on human sympathetic autonomic ganglia. American Journal Pathology 143, 143–153.

Schmidt, R.E., Plurad, D.A., Plurad, S.B., Cogswell, B.E., Diani, A.R., Roth, K.A., 1989. Ultrastructural and immunohistochemical characterization of autonomic neuropathy in genetically diabetic Chinese hamsters. Laboratory Investigation 61, 77–92.

Schmidt, R.E., Dorsey, D.A., Roth, K.A., Parvin, C.A., Hounsom, L., Tomlinson, D.R., 2000. Effect of streptozotocin-induced diabetes on NGF, $P75^{NTR}$ and TrKA content of prevertebral and paravertebral rat sympathetic ganglia. Brain Research 867, 149–156.

Schroer, J.A., Plurad, S.B., Schmidt, R.E., 1992. Fine structure of presynaptic axonal terminals in sympathetic autonomic ganglia of aging and diabetic human subjects. Synapse 12, 1–13.

Statistical Analysis System, 1995. SAS User's Guide: Basic and Statistic. SAS, Cary, NC.

Tracey, W.R., Nakane, M., Pollock, J.S., Förstermann, U., 1993. Nitric oxide synthases in neuronal cells, macrophages and endometrium are NADPH-diaphorases, but present only a fraction of total cellular diaphorase activity. Biochemical and Biophysical Research Communications 195, 1035–1040.

Vincent, S.R., Hope, B.T., 1992. Neurons that say NO. Trends in Neuroscience 15, 108–113.

Willard, M.D., Tvedten, H., Turnwald, G.H., 1994. Small Animal Clinical Diagnosis by Laboratory Methods, second ed. W.B. Saunders Company, Philadelphia.

Worl, J., Wiesand, M., Mayer, B., Greskotter, K.R., Neuhuber, W.L., 1994. Neuronal and endothelial nitric oxide synthase immunoreactivity and NADPH-diaphorase staining in rat and human pancreas: influence of fixation. Histochemistry and Cell Biology 102, 353–364.